



Cite this: *Polym. Chem.*, 2016, 7, 5943

CO₂/pH-responsive particles with built-in fluorescence read-out†

Anne B. Mabire,^a Quentin Brouard,^a Anaïs Pitto-Barry,^a Rebecca J. Williams,^a Helen Willcock,^a Nigel Kirby,^b Emma Chapman^c and Rachel K. O'Reilly^{*a}

A novel fluorescent monomer was synthesized to probe the state of CO₂-responsive cross-linked polymeric particles. The fluorescent emission of this aminobromomaleimide-bearing monomer, being sensitive to protic environments, can provide information on the core hydrophilicity of the particles and therefore indicates the swollen state and size of the particles. The particles' core, synthesized from DEAEMA (*N,N*-diethylaminoethyl methacrylate), is responsive to CO₂ through protonation of the tertiary amines of DEAEMA. The response is reversible and the fluorescence emission can be recovered by simply bubbling nitrogen into the particle solution. Alternate purges of CO₂ and N₂ into the particles' solution allow several ON/OFF fluorescence emission cycles and simultaneous particle swelling/shrinking cycles.

Received 20th July 2016,
Accepted 29th August 2016

DOI: 10.1039/c6py01254j

www.rsc.org/polymers

Introduction

Stimuli-responsive polymers have received great interest in recent years and have been developed for different applications such as nanotechnology, bio-materials and drug delivery.^{1–4} To trigger a response and/or change in properties, external stimuli such as temperature, pH, CO₂ or light can be utilized.^{5–9} The recent interest in CO₂ as a stimulus for responsive materials is due to the natural abundance of this gas and its bio-compatibility. The usage of CO₂-responsive polymers is widely reported to trigger and control self-assembly morphology transitions.^{10–13} These responsive polymers are usually synthesized with monomers containing tertiary amine, amidine, guanidine or imidazole functional groups.^{14–16} These functional groups can all be protonated upon a decrease in pH which in turn can be induced by CO₂. Tertiary amine-containing monomers such as DMAEMA (*N,N*-dimethylaminoethyl methacrylate), DEAEMA and DPAEMA (*N,N*-diisopropylaminoethyl methacrylate) exhibit a pH-responsive behavior, as they can react with strong and weak acids.^{17,18} These pH-responsive monomers are also responsive to CO₂ in water, as CO₂ partially dissolves in water to form an equilibrium with carbonic acid, which is a weak acid that can dissociate into HCO₃[–], CO₃^{2–} and H⁺, allowing protonation of the amine

monomers. The CO₂ response is a reversible process where reversal is carried out by simply bubbling nitrogen or argon in the solution, which displaces carbonic acid and shifts the equilibrium toward the initial pH.¹⁹ CO₂-responsive polymer assemblies can also be obtained *via* encapsulation of amine-bearing small molecules into non-responsive systems such as micelles.²⁰ Further examples of CO₂-responsive materials include the use of CO₂/pH-responsive latexes as Pickering emulsifiers, reported by Morse and co-workers.²¹ The cross-linked latexes were synthesized from DEAEMA, DVB (divinylbenzene) and PEGMA (poly(ethylene glycol methacrylate)) and showed a reversible diameter increase from 230 nm to 590 nm using HCl/KOH or CO₂/N₂ gas purges to change the pH. The protonation of the DEAEMA cross-linked core, using HCl or CO₂, increases the core hydrophilicity, which induces a swelling effect. The deprotonation of DEAEMA *via* N₂ purging or with KOH decreases the hydrophilicity of the core and results in a reduction of the particle diameter back to its original size. Recently, Chen and co-workers also reported the preparation of CO₂-responsive polymeric microgels which are composed of a DEAEMA core covalently stabilized with PEGA (poly(ethylene glycol acrylate)), cross-linked with EGDMA (ethylene glycol dimethacrylate) or BIS (methylene bis(acrylamide)).²² The different microgels obtained showed a reversible size increase upon CO₂ and argon bubbling. Depending on the CO₂ concentration, these microgels can reversibly swell, or swell then collapse.

Fluorescent dyes are of key interest owing to their potential use in drug delivery systems.^{23–25} Liang and co-workers presented the advantages of a responsive and fluorescent combination for bio-medical applications with the preparation of polymeric nanoparticles that are fluorescent, pH-responsive and biocompatible for intracellular imaging and drug

^aUniversity of Warwick, Department of Chemistry, Gibbet Hill Road, Coventry CV4 7AL, UK. E-mail: R.K.O-Reilly@warwick.ac.uk

^bAustralian Synchrotron, 800 Blackburn Road, Clayton, Victoria 3168, Australia

^cBP Exploration Operating Company, Ltd., Chertsey Road, Sunbury-on-Thames, TW16 7BP, UK

†Electronic supplementary information (ESI) available. See DOI: 10.1039/c6py01254j



delivery.²⁶ We previously reported the synthesis of fluorescently labelled proteins and polymers with a dithiomaleimide moiety; a small functional group that does not affect the polymer or protein scaffold.²⁷ This fluorescent functional group was also incorporated into an amphiphilic block copolymer which self-assembled into spherical micelles and can be used in nanomedicine.²⁸ We also recently reported the one-pot synthesis of fluorescent nanogels that were covalently dyed using a dithiomaleimide methacrylate monomer.^{29,30} It was also demonstrated that these particles do not exhibit self-quenching at high concentration unlike commonly used fluorophores such as phloxine B. Dithiomaleimides have been previously demonstrated to be highly fluorescent when the maleimide unit is conjugated to an alkyl thiol,^{27,31} although dithiomaleimides in the presence of an excess of thiol can undergo substitution, which may result in loss of fluorescent properties if substituted with an aromatic thiol.³² To counter this substitution effect and thus the loss of fluorescence, we have recently developed a new class of highly emissive fluorophores, the aminobromomaleimides (ABM).³³ Their fluorescence properties are environment dependent; in protic solvents a loss of fluorescence can be observed. Herein, we report the first synthesis of fluorescent CO₂-responsive polymeric particles by emulsion polymerization. A novel ABM functional fluorescent monomer, present in the particle core, was utilized as a probe of the core hydrophobicity. By simple CO₂ bubbling, the particles become swollen and, as a consequence of the increased hydrophilicity of the particles, their fluorescence drastically decreases. This swelling is reversible by purging the solution with nitrogen and ON/OFF cycles of fluorescence are reproducible with successive CO₂/N₂ purges. PDEAEMA (poly(*N,N*-diethylaminoethyl methacrylate)) was used as the CO₂-responsive core-forming segment, with OEGMA (oligoethylene glycol methacrylate) as the hydrophilic shell-forming block.

Experimental

Materials

Dry solvents were obtained by passing over a column of activated alumina using an Innovative Technologies solvent purification system. DEAEMA was filtered through a plug of alumina prior to use and stored at 4 °C. All other chemicals were purchased from Aldrich, Fluka or Acros and used as received.

Synthetic procedures

Synthesis of the dibromomaleimide methacrylate monomer (DBMMA). To an oven-dried round-bottom flask under an inert nitrogen atmosphere was added triphenyl phosphine (1.03 g, 1 equiv.) and dry THF (35 mL). The mixture was cooled to -78 °C before the dropwise addition of diisopropyl azodicarboxylate (DIAD) (0.769 mL, 1 equiv.). The mixture was stirred for 5 min before adding 2-hydroxyethyl methacrylate (0.475 mL, 1 equiv.), stirred for a further 5 min before adding 2,2-dimethylpropan-1-ol (0.170 g, 0.5 equiv.), and stirred a further 5 min before adding 2,3-dibromomaleimide (1.00 g,

1 equiv.). The reaction was allowed to warm to room temperature while stirring for 18 h. The solvent was removed *in vacuo*, and the crude mixture purified by column chromatography on silica gel using a 1 : 1 mixture of petroleum ether 40–60 °C and dichloromethane, to give the product as a white solid (1.037 g, 73%). The monomer was characterized by ¹H NMR spectroscopy in CDCl₃, ¹³C NMR spectroscopy and mass spectrometry, see ESI.†

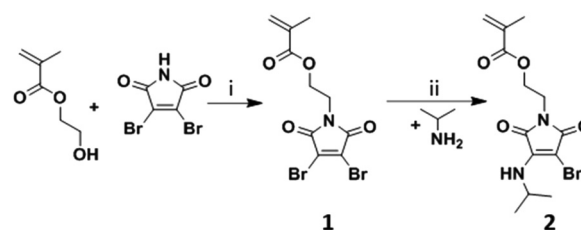
Synthesis of aminobromomaleimide methacrylate (ABMMA). DBMMA (**1**) (1.00 g, 1 equiv.) was dissolved in THF (50 mL). To the solution, sodium carbonate (0.720 g, 2.5 equiv.) was added and stirred. Isopropylamine (0.250 mL, 1.05 equiv.) was added dropwise to the solution, whereby an immediate color change of the solution to yellow and the formation of a white precipitate was observed. Upon complete addition of isopropylamine, the solution was left to stir for 2 h at room temperature. The solvent was removed *in vacuo*, the residue taken up in CH₂Cl₂ (150 mL), washed with water (2 × 150 mL) and dried with MgSO₄. The organic layer was concentrated *in vacuo* and the product purified by column chromatography on silica gel using a 10 : 1 mixture of petroleum ether 40–60 °C and ethyl acetate to yield the product as a yellow-orange crystalline solid (0.88 g, 94%). The product was characterized by ¹H NMR spectroscopy in CDCl₃, ¹³C NMR spectroscopy, mass spectrometry and fluorescence spectroscopy, see ESI.†

General procedure for the synthesis of fluorescent particles. OEGMA (0.11 mmol) was first dissolved in 44 mL of deionised water and then EGDMA (0.126 mmol), and ABMMA (**2**) (0.145 mmol) were dissolved in DEAEMA (13.5 mmol) and added dropwise to the solution. The mixture, whilst stirred, was degassed with nitrogen for 30 min and further heated at 65 °C for 30 min. The initiator, potassium persulfate (KPS) (0.093 mmol), was dissolved in water (1 mL) and degassed with nitrogen before being added to the reaction mixture. The reaction was stirred at 65 °C for 16 h under a nitrogen atmosphere. The particles were purified by exhaustive dialysis (MWCO 3.5 kDa) against deionised water.

Results and discussion

Synthesis and characterization of the fluorescent monomer

The fluorescent monomer containing the ABM functionality was synthesized in two steps, see Scheme 1. First, 2,3-dibromomaleimide methacrylate (DBMMA, **1**) was synthesized by alkyl-



Scheme 1 Synthesis of the ABMMA monomer (**2**). Conditions: (i) PPh₃, DIAD, 2,2-dimethylpropan-1-ol in THF; (ii) Na₂CO₃ in THF.



ation of 2-hydroxyethyl 2-methylprop-2-enoate with 2,3-dibromomaleimide using a modified Mitsunobu reaction procedure reported by Walker.³⁴ The DBMMA monomer (**1**) was then functionalized *via* mono-substitution of the bromine with isopropylamine to obtain an aminobromomaleimide methacrylate (ABMMA, **2**), following a procedure similar to that used for the synthesis of a library of aminomaleimides, previously reported by our group.³³ The monomer presents excitation maxima at 247 nm and 372 nm corresponding to an emission maximum at 482 nm in 1,4-dioxane.

Synthesis and characterization of fluorescent PDEAEMA particles

Fluorescent CO₂/pH-responsive particles were designed with a tertiary amine-bearing monomer (DEAEMA) and the fluorescent ABMMA monomer (**1**), the former allows a pH-response while the latter monomer allows a fluorescence read-out of the particles' state. Particles were synthesized *via* emulsion polymerization in water and the polymerization was initiated by using potassium persulfate (KPS) as the initiator, see Scheme 2. The emulsion polymerization procedure consists of emulsifying an insoluble monomer phase in water in the presence of a stabilizing amphiphilic compound. The amphiphilic compound in this case is OEGMA, which copolymerizes with DEAEMA to form a covalently linked hydrophilic shell. The hydrophobic core is composed of PDEAEMA cross-linked with 1 wt% of EGDMA and 2 wt% of the fluorescent ABMMA monomer (**2**). The tertiary amines of the core-forming block allow a CO₂-responsive behavior while the presence of the ABM allows a built-in fluorescence read-out. Several batches of particles were synthesized. The influence of the OEGMA molecular weight (from 360 Da to 2000 Da) on the particles' size and responsive character was studied. As a control experiment, particles were also synthesized without the fluorescent monomer in order to confirm it does not affect the particles' response to CO₂. The hydrodynamic diameter of the different particles in solution in deionized water was measured by dynamic light scattering (DLS) and it was found that the particles are all in the same size range *ca.* 200 nm, see Table 1 and Fig. 1b, d for the DLS of particles **4** and **8**, see ESI† for particles **3**, **5**, **6** and **7**. The variation of the OEGMA molecular weight or the incorporation of ABMMA did not affect the particles'

Table 1 Characteristics of the different PDEAEMA particles synthesized

No.	OEGMA MW (Da)	Fluorescent?	Hydrodynamic diameter (nm)
3	360	No	185
4	360	Yes	220
5	500	No	235
6	950	No	220
7	2000	No	200
8	2000	Yes	230

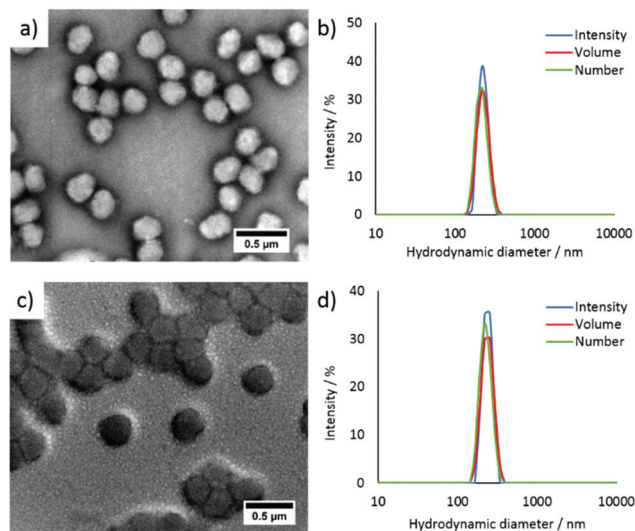
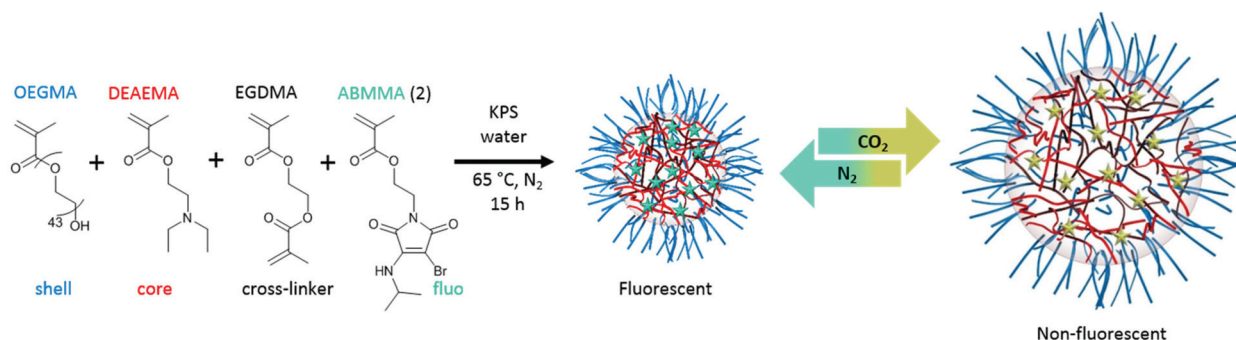


Fig. 1 (a) TEM image of particles **4**, (b) DLS analysis of particles **4**, (c) TEM image of particles **8**, (d) DLS analysis of particles **8**. TEM grids were stained with an aqueous solution of uranyl acetate, see ESI† for more details.³⁵

morphology and size range. The different OEGMA utilized changed the shell's density as the degree of polymerization of OEGMA was kept the same whilst the monomer increased in size. The size of fluorescent particles with different shells (**4** and **8**) was also confirmed by transmission electron microscopy (TEM), see Fig. 1a and c. The particles' spherical morphology was confirmed and the average diameter was measured to be 257 nm for particles **4** and 330 nm for particles **8**. The difference between the



Scheme 2 Synthesis of particles (**8**) *via* emulsion polymerization in water at 65 °C and the reversible particle response upon CO₂ and N₂ bubbling.



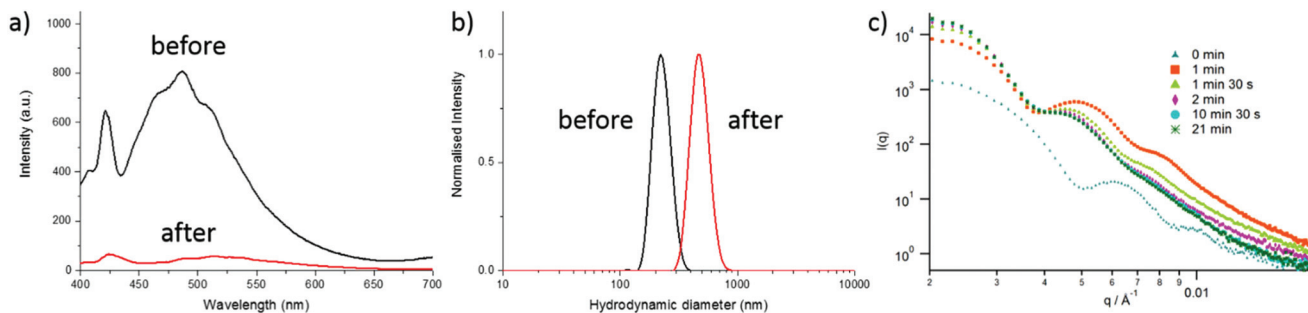


Fig. 2 (a) Fluorescence emission spectra of particles **8** before and after the first CO₂ bubbling, (b) DLS of particles **8** before and after the first CO₂ bubbling, (c) *in situ* size monitoring of particles **3** by SAXS over 21 min of CO₂ bubbling.

DLS hydrodynamic diameter and the TEM average diameter occurs as a consequence of a drying effect. Fluorescence spectroscopy was performed on particles containing the fluorescent monomer (**4** and **8**) in solution in deionized water. The particles both present an emission maximum at 487 nm for an excitation at 375 nm, see Fig. 2a for the emission spectrum of particles **8**.

Particle size monitoring

DLS was utilized to monitor changes in the particle diameter in response to bubbling with CO₂. When CO₂ is bubbled in the particle solution, the amines of PDEAEMA present in the core of the particles become protonated and therefore hydrophilic. Owing to their cross-linked structure, the particles swell and increase in diameter instead of disassembling. A size increase upon CO₂ bubbling was observed for all the particles, see Fig. 2b for particles **8** and ESI† for particles **3**, **4**, **5**, **6** and **7**. For example, the hydrodynamic diameter of particles **3** increased from 185 nm to 390 nm and particles **7** present a diameter increase from 200 nm to 435 nm. The size increase of the non-fluorescent particles with the small molecular weight OEGMA shell (**3**) was also monitored by small angle X-ray light scattering (SAXS) with an *in situ* CO₂ purge, see Fig. 2c. The SAXS data shows an increase of the radius of gyration within minutes. Analysis of the SAXS curves over a period of 21 min indicates an increase of particle size as well as an increase of the dispersity. The initial particles could be analyzed as spherical micelles with really low core dispersity with some polymer coils accounting for the outer hydrated shell.^{36,37} After bubbling CO₂ the dispersity of the core slightly increased (as evidenced by the loss of oscillations in the raw SAXS profiles) and a more pronounced core-shell spherical morphology was observed with an increase of core radius. An initial diameter of 180 nm is observed, and an increase of the diameter is observed over time: after 2 min of bubbling, 255 nm and after 21 min, 280 nm.

Fluorescence emission monitoring

As previously demonstrated by our group, the ABM functional group is sensitive to polar protic environments.³³ Thus, the ABM-bearing monomer should be able to probe the protona-

tion of its environment. Therefore, the increasing hydrophilicity of the core upon CO₂ bubbling should quench the fluorescence emission of the particles. Fluorescence emission of the particles **8** was measured before and after CO₂ bubbling, a drastic decrease of the intensity was observed at 487 nm from 810 a.u. to 50 a.u. (see Fig. 2a). The decrease in fluorescence emission upon CO₂ bubbling was observed under a UV lamp ($\lambda = 345$ nm), see video in ESI.†

Reversibility of the system: CO₂/N₂ purge cycles

To test the reversibility of the system, the particle solution was repeatedly purged with successive cycles of CO₂ and N₂ bubbling. Purge cycles were monitored by fluorescence spectroscopy and DLS. The purging time was kept constant for the entire experiment, CO₂ was bubbled for 15 min and N₂ was bubbled for 30 min. Cycle experiments were performed on fluorescent particles with the denser OEGMA shell (**8**). The hydrodynamic diameter and the fluorescence emission at 487 nm of the particles (**8**) were measured after each CO₂ or N₂ purge. As shown in Fig. 3, the size of the particles alternatively increases and decreases six times. Similarly the emission intensity is reversibly quenched eight times (Fig. 4). Although

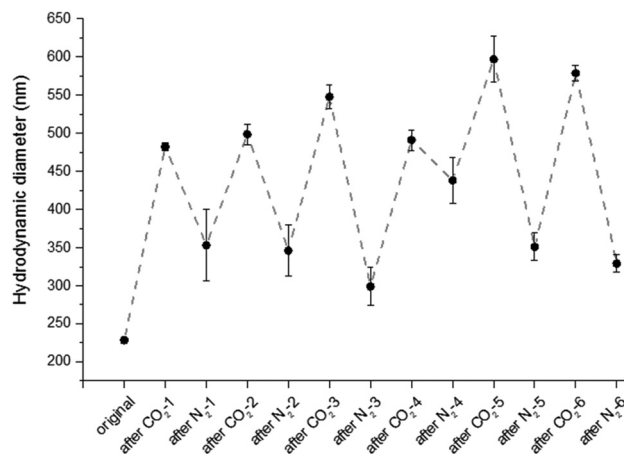


Fig. 3 Hydrodynamic diameter of the particles (**8**) in deionized water measured after each gas purge.



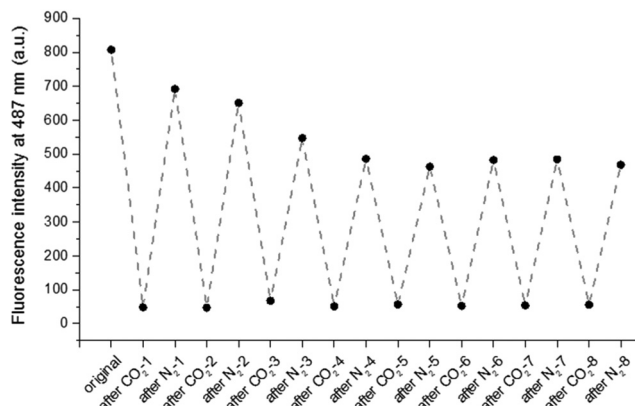


Fig. 4 Fluorescence emission intensity at 487 nm measured of the particles (8) in deionized water after each gas purge.

particles with a less dense shell (3, 4, 5, 6) can swell with CO₂, they are unable to collapse upon N₂ bubbling. For example, particles 5 exhibit a diameter of 235 nm before bubbling, 430 nm after CO₂ bubbling and 1000 nm after N₂ purge. This irreversible swelling occurs as a consequence of the density of the shell that cannot counter the effect of core chains that irreversibly penetrate the shell during the first protonation. These hydrophobic chains get trapped in the shell when the particles shrink and their presence promotes inter-particle interactions, which leads to the formation of uncontrolled large aggregates. The formation of aggregates is significantly reduced with a denser shell made of OEGMA with a molecular weight of 2000 Da.

Conclusions

In conclusion, we have presented the synthesis of fluorescent CO₂-responsive cross-linked polymeric particles. The fluorescent dye was incorporated in the core in the form of a novel fluorescent monomer containing an ABM functional group while the CO₂-responsive character was introduced by the presence of tertiary amines. These particles swell as the core is made hydrophilic by bubbling CO₂ into the solution. This change of local hydrophobic character then induces a decrease in ABM fluorescence intensity. Thus, the fluorescence intensity can be used to probe the particle core hydrophobicity and particle size.

Acknowledgements

The authors thank Dr Dafni Moatsou and Dr Mathew Robin for helpful discussions, BP and the EPSRC for funding.

Notes and references

1 M. R. Hill, E. J. MacKrell, C. P. Forsthoefel, S. P. Jensen, M. Chen, G. A. Moore, Z. L. He and B. S. Sumerlin, *Biomacromolecules*, 2015, **16**, 1276–1282.

2 I. Cobo, M. Li, B. S. Sumerlin and S. Perrier, *Nat. Mater.*, 2015, **14**, 143–159.

3 P. Theato, B. S. Sumerlin, R. K. O'Reilly and I. I. T. H. Epps, *Chem. Soc. Rev.*, 2013, **42**, 7055–7056.

4 C.-Y. Chen and H.-L. Wang, *Macromol. Rapid Commun.*, 2014, **35**, 1534–1540.

5 M. I. Gibson and R. K. O'Reilly, *Chem. Soc. Rev.*, 2013, **42**, 7204–7213.

6 S. Dai, P. Ravi and K. C. Tam, *Soft Matter*, 2008, **4**, 435–449.

7 X. Xiao, S. He, M. Dan, F. Huo and W. Zhang, *Chem. Commun.*, 2014, **50**, 3969–3972.

8 B. W. Liu, H. Zhou, S. T. Zhou, H. J. Zhang, A. C. Feng, C. M. Jian, J. Hu, W. P. Gao and J. Y. Yuan, *Macromolecules*, 2014, **47**, 2938–2946.

9 B. A. Abel, M. B. Sims and C. L. McCormick, *Macromolecules*, 2015, **48**, 5487–5495.

10 A. Darabi, P. G. Jessop and M. F. Cunningham, *Chem. Soc. Rev.*, 2016, **45**, 4391–4436.

11 Q. Yan and Y. Zhao, *Chem. Commun.*, 2014, **50**, 11631–11641.

12 S. Lin and P. Theato, *Macromol. Rapid Commun.*, 2013, **34**, 1118–1133.

13 E. Girard, T. Tassaing, J.-D. Marty and M. Destarac, *Chem. Rev.*, 2016, **116**, 4125–4169.

14 Q. Yan, R. Zhou, C. Fu, H. Zhang, Y. Yin and J. Yuan, *Angew. Chem., Int. Ed.*, 2011, **50**, 4923–4927.

15 P. Schattling, I. Pollmann and P. Theato, *React. Funct. Polym.*, 2014, **75**, 16–21.

16 J. Y. Quek, P. J. Roth, R. A. Evans, T. P. Davis and A. B. Lowe, *J. Polym. Sci., Part A: Polym. Chem.*, 2013, **51**, 394–404.

17 S. Shahalom, T. Tong, S. Emmett and B. R. Saunders, *Langmuir*, 2006, **22**, 8311–8317.

18 J. Pinaud, E. Kowal, M. F. Cunningham and P. Jessop, *ACS Macro Lett.*, 2012, **1**, 1103–1107.

19 Y. Hoshino, K. Imamura, M. Yue, G. Inoue and Y. Miura, *J. Am. Chem. Soc.*, 2012, **134**, 18177–18180.

20 S. Salentinig, P. Jackson and A. Hawley, *Macromolecules*, 2015, **48**, 2283–2289.

21 A. J. Morse, S. P. Armes, K. L. Thompson, D. Dupin, L. A. Fielding, P. Mills and R. Swart, *Langmuir*, 2013, **29**, 5466–5475.

22 Y. Chen, T. Zhao, B. Wang, D. Qiu and N. Ma, *Langmuir*, 2015, **31**, 8138–8145.

23 M. P. Robin and R. K. O'Reilly, *Polym. Int.*, 2015, **64**, 174–182.

24 H. Wang, M. Xu, M. Xiong and J. Cheng, *Chem. Commun.*, 2015, **51**, 4807–4810.

25 J.-K. Y. Tan, J. L. Choi, H. Wei, J. G. Schellinger and S. H. Pun, *Biomater. Sci.*, 2015, **3**, 112–120.

26 S. Li, K. Hu, W. Cao, Y. Sun, W. Sheng, F. Li, Y. Wu and X.-J. Liang, *Nanoscale*, 2014, **6**, 13701–13709.

27 M. P. Robin, P. Wilson, A. B. Mabire, J. K. Kiviahio, J. E. Raymond, D. M. Haddleton and R. K. O'Reilly, *J. Am. Chem. Soc.*, 2013, **135**, 2875–2878.



- 28 M. P. Robin, A. B. Mabire, J. C. Damborsky, E. S. Thom, U. H. Winzer-Serhan, J. E. Raymond and R. K. O'Reilly, *J. Am. Chem. Soc.*, 2013, **135**, 9518–9524.
- 29 M. P. Robin, J. E. Raymond and R. K. O'Reilly, *Mater. Horiz.*, 2015, **2**, 54–59.
- 30 M. P. Robin and R. K. O'Reilly, *Chem. Sci.*, 2014, **5**, 2717–2723.
- 31 Z.-L. Li, L. Sun, J. Ma, Z. Zeng and H. Jiang, *Polymer*, 2016, **84**, 336–342.
- 32 A. B. Mabire, M. P. Robin, H. Willcock, A. Pitto-Barry, N. Kirby and R. K. O'Reilly, *Chem. Commun.*, 2014, **50**, 11492–11495.
- 33 A. B. Mabire, M. P. Robin, W.-D. Quan, H. Willcock, V. G. Stavros and R. K. O'Reilly, *Chem. Commun.*, 2015, **51**, 9733–9736.
- 34 M. A. Walker, *J. Org. Chem.*, 1995, **60**, 5352–5355.
- 35 J. P. Patterson, M. P. Robin, C. Chassenieux, O. Colombani and R. K. O'Reilly, *Chem. Soc. Rev.*, 2014, **43**, 2412–2425.
- 36 D. B. Wright, J. P. Patterson, A. Pitto-Barry, A. Lu, N. Kirby, N. C. Gianneschi, C. Chassenieux, O. Colombani and R. K. O'Reilly, *Macromolecules*, 2015, **48**, 6516–6522.
- 37 D. B. Wright, J. P. Patterson, A. Pitto-Barry, P. Cotanda, C. Chassenieux, O. Colombani and R. K. O'Reilly, *Polym. Chem.*, 2015, **6**, 2761–2768.

